

Fast evolving size of early-type galaxies at $z > 2$ and the role of dissipationless (*dry*) merging

A. Cimatti^{1*}, C. Nipoti¹, P. Cassata²

¹Università di Bologna, Dipartimento di Astronomia, Via Ranzani 1, I-40127, Bologna, Italy

²Laboratoire d'Astrophysique de Marseille - LAM, Université d'Aix-Marseille & CNRS, UMR7326, 38 rue F. Joliot-Curie, F-13388 Marseille Cedex 13, France

Accepted 2012 xxx xxx. Received 2011 XX XX; in original form 2011 XX XX

ABSTRACT

We present the analysis of a large sample of early-type galaxies (ETGs) at $0 < z < 3$ aimed at tracing the cosmic evolution of their size and compare it with a model of pure dissipationless (*dry*) merging in the Λ CDM framework. The effective radius R_e depends on stellar mass \mathcal{M} as $R_e(\mathcal{M}) \propto \mathcal{M}^\alpha$ with $\alpha \sim 0.5$ at all redshifts. The redshift evolution of the mass- or SDSS-normalized size can be reproduced as $\propto (1+z)^\beta$ with $\beta \sim -1$, with the most massive ETGs possibly showing the fastest evolutionary rate ($\beta \sim -1.4$). This size evolution slows down significantly to $\beta \sim -0.6$ if the ETGs at $z > 2$ are removed from the sample, suggesting an accelerated increase of the typical sizes at $z > 2$, especially for the ETGs with the largest masses. A pure *dry* merging Λ CDM model is marginally consistent with the average size evolution at $0 < z < 1.7$, but predicts descendants too compact for $z > 2$ progenitor ETGs. This opens the crucial question on what physical mechanism can explain the accelerated evolution at $z > 2$, or whether an unclear observational bias is partly responsible for that.

Key words: galaxies: formation – galaxies: evolution – galaxies: ellipticals and lenticulars, cD

1 INTRODUCTION

Early-type galaxies (ETGs) are important probes of structure formation and massive galaxy evolution. At $0 < z < 1$, the ETG stellar mass function shows a *downsizing* evolution apparently difficult to reproduce with the current models of galaxy formation, with the majority of massive ETGs ($\mathcal{M} > 10^{11} M_\odot$) already in place at $z \approx 0.7$, (Pozzetti et al. 2010 and references therein). At $z > 1$, the information is still incomplete, but *bona fide* ETGs have been identified up to $z \sim 2.5$ (e.g. Kriek et al. 2006; Cimatti et al. 2008 and references therein). These high- z ETGs are characterized by old stars (1-3 Gyr), e -folding decaying star formation timescales $\tau \sim 0.1$ – 0.3 Gyr, low specific star formation rates ($\text{SSFR} < 10^{-2} \text{ Gyr}^{-1}$), low dust extinction, large stellar masses ($\mathcal{M} > 10^{11} M_\odot$), spheroidal morphologies (although some of these systems have a disk-like component; van der Wel et al. 2011), and number densities growing rapidly from $z > 3$ to $z \sim 1$ (e.g. Fontana et al. 2009; Domínguez-Sánchez et al. 2011; Brammer et al. 2011).

A puzzling property of ETGs at $z > 1$ is that they have smaller sizes, down to effective radii $R_e < 1$ kpc, and correspondingly higher internal mass densities than present-day

ETGs with the same mass (e.g. Daddi et al. 2005; Trujillo et al. 2006; van der Wel et al. 2008; Cimatti et al. 2008; Buitrago et al. 2008; Saracco, Longhetti & Andreon 2009; Williams et al. 2010; Cassata et al. 2011; Damjanov et al. 2011; Newman et al. 2011, and references therein). It is not clear yet whether the environment plays (e.g. Papovich et al. 2011; Cooper et al. 2011) or not (e.g. Rettura et al. 2010) a role in the ETG size evolution. The few available measurements of stellar velocity dispersions are consistent with those expected from the ETG sizes and confirm that these systems are truly massive (Cenarro et al. 2009; Cappellari et al. 2009; Onodera et al. 2010; van Dokkum, Kriek & Franx 2009; van de Sande et al. 2011). Several models have been proposed to explain the size–mass evolution, including dissipationless (*dry*) major and minor merging, adiabatic expansion driven by stellar mass loss and/or strong feedback, and smooth stellar accretion (e.g. Khochfar & Silk 2006; Bournaud, Jog & Combes 2007; Fan et al. 2008; Nipoti et al. 2003, 2009a, 2009b; Naab et al. 2009; Hopkins et al. 2009; Oser et al. 2011). However, the global picture is far from being clear. In this paper, we exploit a large sample of ETGs in order to investigate the evolution of their size as a function of redshift and mass, and compare it with the predictions of cosmological models of structure formation.

* E-mail: a.cimatti@unibo.it

Table 1. ETG subsamples

Sample	N	Redshift	Age	Ref.
SDSS	59500	$0 < z < 0.4$	yes	1
COSMOS/zCOSMOS	950	$0 < z < 1$	no	2
GOODS-N+S	469	$0 < z^* < 2$	yes	3
Literature	465	$0.2 < z < 2.7$	no	4
GMASS	45	$1.4 < z^* < 3$	no	5
COSMOS	12	$1.4 < z^* < 1.8$	yes	6
XMMU J2235-2557	11	$z=1.39$	yes	7
K20-0055	9	$0.7 < z < 1.2$	yes	8
POWIR	6	$1.2 < z^* < 1.8$	no	9
K20	4	$1.6 < z < 1.9$	yes	10
1255-0	1	$z = 2.186$	yes	11
FW-4871	1	$z = 1.902$	yes	12

z^* : a fraction of redshifts is photometric, Age: available stellar ages. 1. Hyde & Bernardi 2009, 2. <http://cosmos.astro.caltech.edu/data/index.html>, Scarlata et al. 2007, Moresco et al. 2010, 3. Cassata et al. 2011, 4. Damjanov et al. 2011, 5. Cassata et al. 2008, 6. Mancini et al. 2010, 7. Strazzullo et al. 2010, 8. di Serego Alighieri et al. 2005, 9. Carrasco, Conselice & Trujillo 2010 ($n_{Sersic} > 2$), 10. Cimatti et al. 2004, 11. van Dokkum et al. 2009, 12. van Dokkum & Brammer 2010.

2 THE SAMPLE

In order to improve statistically on previous studies, we selected a large sample of 1975 ETGs at $0.2 < z < 3$ by collecting data from the literature and public data, requiring the availability of spectroscopic redshifts (or high-quality photometric redshifts for $z > 1.4$), stellar masses, sizes (R_e) and, when possible, age of the stellar population (see Tab. 1). The ETGs in the different subsamples share the global property to have been originally selected based on the combination of colors, spectra (or sometimes also SSFR) typical of old/passive galaxies with the confirmation of spheroidal (E/S0) morphology, or vice versa. We recall that selection criteria for ETGs are strongly correlated, with up to $\sim 85\%$ color/spectra-selected ETGs being also morphologically E/S0 (e.g. Renzini 2006 and references therein). The ETG sizes were generally measured in the observed-frame red-optical for low-/intermediate-redshift samples and/or in the near-infrared for higher redshifts, i.e. typically sampling the rest-frame optical region at all redshifts. Recently, Damjanov et al. (2011) and Cassata et al. (2011) have shown that the sizes measured in the rest-frame UV and in the optical correlate very strongly with each other, thus excluding substantial biases dependent on the wavelength at which the size was measured. The SDSS sample of Hyde & Bernardi (2009) was included as the reference sample at $z \sim 0$.

The different subsamples were harmonized to the same cosmology ($H_0 = 70 \text{ km s}^{-1} \text{ Mpc}^{-1}$, $\Omega_m = 0.3$, $\Omega_\Lambda = 0.7$), and the stellar masses and ages rescaled to the Maraston (2005) stellar population synthesis models with the Chabrier Initial Mass Function (IMF) by using empirical scaling relations of Pforr et al. (2012).

Based on the information available in the literature, the stellar mass completeness of most subsamples is $\log \mathcal{M}_{comp}/M_\odot = 10.5$ at all redshifts. However, a few subsamples have $\log \mathcal{M}_{comp}/M_\odot \sim 10.8 - 11$: GN/DEIMOS (from Damjanov et al. 2011) and zCOSMOS at $z < 1.3$,

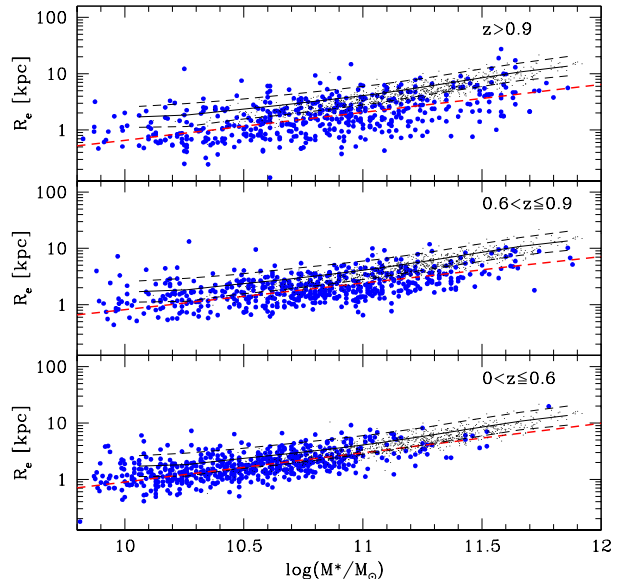


Figure 1. The size – stellar mass relation for $\log \mathcal{M}/M_\odot > 10.5$. Black and blue symbols indicate SDSS and non-SDSS ETGs respectively. Only SDSS ETGs older than 10 Gyr are shown in order to avoid excessive crowding. The black solid line shows the size–mass relation of Shen et al. (2003) and its $\pm 1\sigma$ scatter (dashed black lines). Red dashed lines: best fit relations using $R_e \propto \mathcal{M}^\alpha$.

MUNICS, K20, Mancini et al. (2010) and van Dokkum et al. (2008) at $1.3 < z < 2$, Cassata et al. (2011) and van Dokkum et al. (2008) at $z > 2$. The final sample was reduced to 1080 galaxies in order to avoid mass incompleteness effects (see Section 4 for details).

3 THE SIZE – MASS RELATION

Figure 1 shows the size–mass relation in three redshift ranges with a comparable number of galaxy in each bin. A power-law fit, $R_e \propto \mathcal{M}^\alpha$, applied to non-SDSS ETGs with $\log \mathcal{M}/M_\odot > 10.5$ provides $\alpha = 0.52 \pm 0.05$, 0.47 ± 0.04 , 0.50 ± 0.04 from low to high redshift in the three bins of Fig. 1, with α basically independent of redshift. For instance, the ETGs with $z > 2$ have $\alpha = 0.45 \pm 0.11$. This result is consistent with recent works (Damjanov et al. 2011; Newman et al. 2011), and does not depend significantly on the choice of the redshift bin limits or the minimum stellar mass cuts. In comparison, the SDSS ETGs with $\log \mathcal{M}/M_\odot > 10.5$ have $\alpha = 0.58 \pm 0.01$, consistent with Shen et al. (2003).

4 THE SIZE – REDSHIFT RELATION

Fig. 2 shows the redshift evolution of the ETG size in two complementary ways: the mass-normalized radius ($R_e(z)/\mathcal{M}_{11}^\alpha$, where $\mathcal{M}_{11} = \mathcal{M}/10^{11} M_\odot$, adopting $\alpha = 0.55$ as representative value), and radius normalized to the average size of SDSS ETGs ($R_e(z)/R_e(\text{SDSS})$) in three mass bins. Both quantities are useful to derive the size evolution independently of the correlation between R_e and \mathcal{M} . The evolution is parametrized by the usual functional form

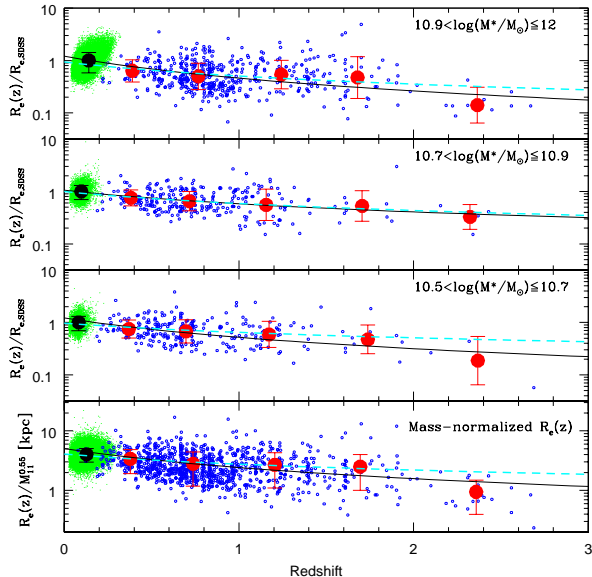


Figure 2. *Bottom panel:* the mass-normalized radius ($R_e/M_{11}^{0.55}$) of ETGs with $\log \mathcal{M}/M_\odot > 10.5$ as a function of z . *Top three panels:* the fractional radius (relative to SDSS; $\langle R_e(SDSS) \rangle = 2.51, 3.10, 5.61$ kpc). In all panels, green and blue small symbols indicate individual SDSS and non-SDSS ETGs respectively, whereas the large black and red filled circles are the average values ($\langle R_e/R_e(SDSS) \rangle$) of SDSS and non-SDSS respectively, each with the $\pm 1\sigma$ scatter. The black solid line is the best fitting function to the red and black points. The redshift bins adopted for the non-SDSS ETGs in this figure are $0 < z < 0.5$, $0.5 < z < 1$, $1 < z < 1.5$, $1.5 < z < 2$, $2 < z < 3$. The cyan dashed lines show the best fits for the case of ETGs with $z < 2$ (redshift bins: $0 < z < 0.3$, $0.3 < z < 0.6$, $0.6 < z < 1$, $1 < z < 1.5$, $1.5 < z < 2$).

size $\propto (1+z)^\beta$. Clearly, this parametrization does not mean that *all* high- z ETGs are the direct progenitors of *all* low- z ETGs because these galaxies evolve in the redshift range $0 < z < 3$ through several processes and increase their number density and mass, but it has simply the statistical meaning of indicating how the *typical* sizes compare at different redshifts.

In order to mitigate the potential effects of stellar mass incompleteness, for each mass bin of Fig.2 (top three panels), the galaxies with $\mathcal{M} < \mathcal{M}_{comp}(z)$ were removed from each subsample. Thus, each mass bin is always complete down to the minimum mass of the bin. For instance, the ETGs with $\mathcal{M} < 10^{11} M_\odot$ at $z \geq 1$ and $\mathcal{M} < 10^{10.6} M_\odot$ at $z \geq 2$ have been excluded from the zCOSMOS and the Cassata et al. (2011) sample respectively.

For the mass-normalized radius (Fig.2, bottom panel), we derive $\beta = -1.06 \pm 0.14$ (-1.24 ± 0.15) for $\log \mathcal{M}/M_\odot > 10.5$ (10.9), in agreement with the literature (Damjanov et al. 2011, Newman et al. 2011). This result is stable against changing α between 0.4 and 0.7, the boundaries of the redshift bins, and the minimum stellar mass. The consistency of the $R_e \propto \mathcal{M}^\alpha$ and $(R_e/M_{11}^\alpha) \propto (1+z)^\beta$ relations with previous results confirms that our sample, despite its somehow heterogeneous composition, can be reliably used to perform further detailed studies.

Fig. 2 (top three panels) shows R_e normalized to

$R_e(SDSS)$. For the three bins of increasing mass, we derive $\beta = -1.23 \pm 0.15$, -0.87 ± 0.14 and -1.39 ± 0.13 . This suggests that β does not significantly depend on stellar mass, although a steepening is suggested in the most massive bin. These results are stable, within the statistical uncertainties, against changes in the minimum stellar mass in the lowest mass bin, in the boundaries of the mass bins, and in the minimum age of the SDSS ETGs.

Fig. 2 also shows that the ETG size growth rate seems to increase significantly at high redshift, suggesting a slower evolution at $z < 2$. For the mass-normalized radius (bottom panel), β becomes -0.57 ± 0.15 if the ETGs at $z_{cut} > 2$ are excluded. Similarly for $R_e/R_e(SDSS)$, β becomes $\beta = -0.73 \pm 0.14$, -0.76 ± 0.13 and -0.75 ± 0.14 if ETGs at $z > 2$ are excluded in the three bins of increasing mass. We note that the flattening is particularly pronounced and significant in the bin of largest masses. The flattening of β is also present, within the statistical uncertainties, against changing the limits of the redshift bins if we cut ETGs around $1.5 < z_{cut} < 2$. For instance, if the ETGs with $z_{cut} > 1.5$ (1.7) are excluded in the bin with $\log \mathcal{M}/M_\odot > 10.9$, we derive $\beta = -0.95$ (-0.72) ± 0.15 . The overall results presented in this section do not change if median values are used instead of the average ones, nor if the SDSS data points are excluded.

The potential role of the so-called progenitor bias (e.g. Saglia et al. 2010 and references therein) has been assessed through an *age filtering* by comparing the size of ETGs having ages compatible with the cosmic time passed from high- z to low- z . For a given redshift range $z_1 < z < z_2$ and average redshift \bar{z} , we estimated β by comparing the average size of the ETGs (having an average age $t_{age}(\bar{z}) \pm \sigma_{t(z)}$) with the size of SDSS ETGs with ages at z_0 between $[t_{age}(\bar{z}) - \sigma_{t(z)}] + \tau(z - z_0)$ and $[t_{age}(\bar{z}) + \sigma_{t(z)}] + \tau(z - z_0)$, where $\tau(z - z_0)$ is the cosmic time passed from z to z_0 . Based on this approach, no significant or systematic changes of β have been found for a variety of tested redshift ranges. For example, for ETGs with $\log \mathcal{M}/M_\odot > 10.9$ at $0.7 < z < 1.3$, we derive $\beta = -1.06 \pm 0.2$ and $\beta = -0.97 \pm 0.2$ respectively with and without applying the above age filtering. Similarly, if we select the most distant ETGs ($1.8 < z < 3$), we obtain $\beta = -1.29 \pm 0.2$ and $\beta = -1.23 \pm 0.2$. If we take these results at face value, this implies that most of the $R_e(z)$ evolution is unlikely to be the result of a progenitor bias due to high- z ETGs being preferentially selected to be redder and more compact than lower- z younger and larger ETGs missed at high- z . However, we recall that, due to the heterogeneous estimates of the stellar ages in our sample, this result should be confirmed with larger and more homogeneous samples. On the other hand, we note that large ETGs are indeed absent at $1.4 < z < 3$ in the GMASS subsample (Fig. 2), that is selected based solely on morphology irrespective of colours (Cassata et al. 2008).

5 COMPARISON WITH A Λ CDM MODEL

Dissipationless (*dry*) merging is one of the few mechanisms known to make galaxies less compact (e.g., Nipoti et al. 2003; Naab et al. 2009), so it is often invoked to explain the observed size evolution of ETGs. Here we briefly address the question of whether the observed size evolution is consistent with the merger histories of concordance Λ cold dark matter

(Λ CDM) cosmology. For this purpose, we use the Λ CDM-based merger models presented in Nipoti et al. (2012, hereafter N12), which are such that the variation in surface-mass density is maximized, because dissipative effects are neglected. In particular, we adopt here model B of N12, which is the most strongly evolving of their models, so the predicted size evolution must be considered an upper limit. Here we briefly describe the main properties of the model, but we refer the reader to N12 for details. For an observed ETG with measured stellar mass \mathcal{M} and effective radius R_e , the model allows to calculate the redshift evolution of \mathcal{M} and R_e via analytic functions calibrated on N -body simulations. The galaxy is first assigned a halo mass using the redshift-dependent stellar to halo mass relation of Behroozi, Conroy, & Wechsler (2010). The halo growth-history is then computed using Fakhouri et al. (2010) fit to halo merger histories in the Millenium I and II simulations (Springel et al. 2005; Boylan-Kolchin et al. 2009). The associated growth of \mathcal{M} is obtained by assigning stellar mass to satellite halos with Behroozi et al. (2010) recipe, and considering only mergers with mass ratio >0.03 (to exclude cases with too long merging time). Finally, the corresponding variation in R_e is computed using analytic functions verified with N -body simulations of minor and major dry mergers between spheroids. For observed high- z ETGs, we compute the predicted $\mathcal{M}(z)$ and $R_e(z)$ up to $z = 0.14$, which is the average redshift of massive ($\log \mathcal{M}/M_\odot > 10.9$) SDSS ETGs. The evolution in the \mathcal{M} - R_e plane is shown in Fig. 3, taking as progenitors the observed ETGs with $2 < z < 3$ ($\langle z \rangle \simeq 2.4$) and those with $1.5 < z < 2$ ($\langle z \rangle \simeq 1.7$). In both cases the present-day descendants tend to be more compact than real $z \sim 0$ ETGs, but the deviation from the SDSS \mathcal{M} - R_e relation is larger than the observed scatter ($\sim 0.15 \log R_e$ at given \mathcal{M}) only when $z \sim 2.4$ progenitors are considered: the $z \sim 0$ descendants have median vertical offset from the SDSS best-fit $\Delta \log R_e \simeq -0.3(-0.1)$ for $z \sim 2.4(1.7)$ progenitors. In the case of $z \sim 2.4$ progenitors, also the $z = 1$ model descendants are more compact than real $z \sim 1$ ETGs. We conclude that the $z > 2$ ETGs are so compact that, even according to extreme pure *dry*-merger models, their low- z descendants are predicted to be significantly more compact than present-day ETGs. On the other hand, the milder size evolution observed since $z \sim 1.7$ is marginally consistent with Λ CDM *dry*-merger models, though the model descendants are distributed in the \mathcal{M} - R_e plane with larger scatter than the observed ETGs (see also N12). An additional problem is the presence, among the predicted $z \sim 0$ descendants, of outliers, i.e. galaxies in regions of the \mathcal{M} - R_e in which there are no SDSS ETGs: for instance, three model galaxies with $\log \mathcal{M}/M_\odot \sim 12$ and $R_e > 70$ kpc, and a model galaxy with $\log \mathcal{M}/M_\odot \sim 11.5$ and $R_e \sim 0.3$ kpc (Fig. 3). We recall here that the existence of compact low- z ETGs with sizes and masses comparable to those of compact ETGs at $z > 2$ is somehow unclear, with some results showing an absence of such galaxies (e.g. Taylor et al. 2010) and others finding a few candidates (e.g. Shih & Stockton 2011; Valentinuzzi et al. 2010). Do our results necessarily imply that dry merging alone cannot explain the observed size evolution? In principle it could be the case that dry mergers are responsible for the whole size evolution, but the actual rate of mergers is higher than predicted. This hypothesis can be tested by further comparison with observations. A first constraint comes

from the observed redshift evolution of the ETG stellar mass function. Let us take, for instance, the model describing the evolution of the $z \sim 1.7$ ETGs. At each $z \leq 1.7$ we select only model galaxies with $\log \mathcal{M}/M_\odot \geq 10.9$ and for this subsample we measure the average stellar mass $\langle \log \mathcal{M} \rangle$. The redshift variation of $\langle \log \mathcal{M} \rangle$ is found to be well represented by the fit $\langle \log \mathcal{M}/M_\odot \rangle(z) = 11.57 - 0.15z$, i.e. the average mass increase by $\sim 30\%$ (70%) from $z = 0.7(1.5)$ to the present. This is compatible with observed evolution of the ETG stellar mass function at $0 < z < 1$ (e.g. Pozzetti et al. 2010). Another testable feature of the model is the predicted merger rate. Let us define major(minor) mergers those with mass ratio $>(<)/4$. The predicted number of major mergers per unit time dN_m/dt decreases for decreasing z (see Fakhouri et al. 2010): for our model ETGs we get, on average, $dN_m/dt \sim 0.13(0.23) \text{ Gyr}^{-1}$ at $z \sim 0.55(1.15)$. These rates are higher by a factor of ~ 2 than estimated observationally at similar z by Bundy et al. (2009; see also Lotz et al. 2011), indicating that the considered model might be extreme also in this respect. In the model, both major and minor mergers contribute significantly to the growth of stellar mass (for instance, $\sim 50\%$ each between $z = 1.5$ and $z = 0$), so, at least within Λ CDM, massive ETGs do not accrete most of their mass in very minor mergers, which would be more effective in increasing the galaxy size. The above arguments suggest that other processes not included in the model should contribute significantly to the size evolution. Unfortunately, at the moment the proposals for additional mechanisms are not very promising: Fan et al. (2008) envisaged that feedback from QSOs could play a role, but also this scenario is not without problems (Ragone-Figueroa & Granato 2011).

6 CONCLUSIONS

The analysis of a large sample of ETGs at $0 < z < 3$ shows that their size evolves independently of stellar mass and possibly faster at $z > 2$ (especially for ETGs with the largest masses). The interpretation of this result is not straightforward as the available information does not allow us to assess if this is an observational bias (e.g. large ETGs with low surface brightness are missed in high- z samples), or it is an intrinsic change in the evolutionary pattern implying a very rapid growth of ETGs from $z > 2$ to lower redshifts. We explored the possibility of pure *dry* merging as the dominant growth mechanism within the Λ CDM framework, and found that this scenario is marginally consistent with the average size evolution at $0 < z < 1.7$, but predicts descendants too compact for $z > 2$ progenitor ETGs. Further studies and larger samples of ETGs at $z > 1.5$, which will be obtained with future wide-field surveys (e.g. *Euclid*, Laureijs et al. 2011), will shed light on these open questions.

7 ACKNOWLEDGEMENTS

We thank M. Bernardi, M. Moresco and V. Strazzullo for providing their data, J. Pforr and C. Maraston for providing their scaling relations, E. Daddi and A. Renzini for useful discussion, the COSMOS/zCOSMOS teams for making the data available to the community, and the anonymous referee

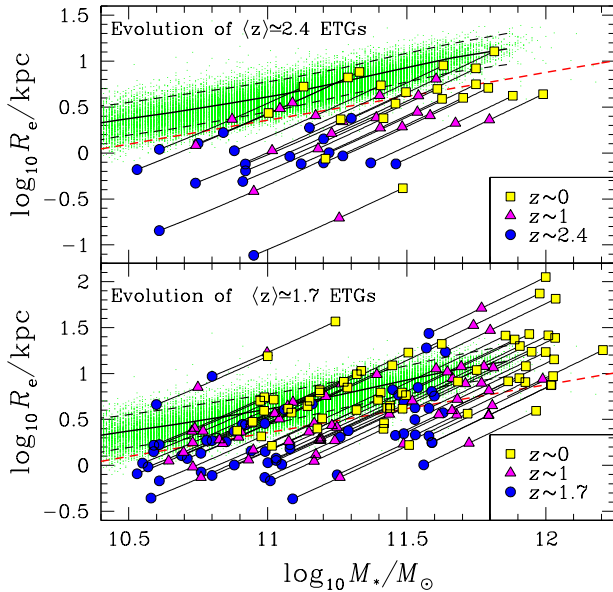


Figure 3. Redshift evolution of ETGs in the stellar mass-effective radius plane, as predicted by the *dry*-merger Λ CDM model described in Section 5. The progenitors (circles) are the ETGs observed at $2 < z < 3$ ($\langle z \rangle \simeq 2.4$, upper panel) and those observed at $1.5 < z < 2$ ($\langle z \rangle \simeq 1.7$, lower panel). The predicted descendants at $z = 1$ and $z = 0.14$ are represented, respectively, by the triangles and the squares. For comparison we plot SDSS ETGs (green dots) and the local SDSS best-fit with its observed scatter (black solid and dashed curves; Shen et al. 2003). The red dashed lines indicate the best-fits for ETGs observed at $0.8 < z < 1.2$.

for the constructive comments. AC is supported by grants ASI-Uni. Bologna-Astronomy Dept. I/039/10/0 and PRIN MIUR 2008. CN is supported by grant PRIN MIUR 2008. Paolo Cassata acknowledges support from ERC grant ERC-2010-AdG-26107-EARLY.

REFERENCES

- Behroozi P. S., Conroy C., Wechsler R. H., 2010, ApJ, 717, 379
 Bournaud F., Jog C.J. & Combes F. 2007, A&A, 476, 1179
 Boylan-Kolchin M., Springel V., White S. D. M., Jenkins A., Lemson G., 2009, MNRAS, 398, 1150
 Brammer G.B. et al. 2011, ApJ, 739, 24
 Buitrago F., Trujillo I., Conselice C., Bouwens R.J., Dickinson M., Yan H. 2008, ApJ, 687, L61
 Bundy K., Fukugita M., Ellis R. S., Targett T. A., Belli S., Kodama T., 2009, ApJ, 697, 1369
 Cappellari M. et al. 2009, ApJ, 704, L34
 Carrasco E.R., Conselice C.J., Trujillo I. 2010, MNRAS, 405, 2253
 Cassata P. et al. 2008, A&A, 483, L39
 Cassata P. et al. 2011, ApJ, 743, 96
 Cenarro A.J., Trujillo I. 2009, ApJ, 696, L43
 Cimatti A. et al. 2004, Nature, 430, 184
 Cimatti, A. et al. 2008, A&A, 482, 21
 Cooper M.C. et al. 2011, ApJ, in press (arXiv:1109.5698)
 Daddi, E. et al. 2005, ApJ, 626, 680
 Damjanov I. et al. 2011, ApJ, 739, L44
 di Serego Alighieri S. et al. 2005, A&A, 442, 125
 Domínguez Sánchez, H. et al. 2011, MNRAS, 417, 900
 Fakhouri O., Ma C.-P., Boylan-Kolchin M., 2010, MNRAS, 406, 2267
 Fan L., Lapi A., De Zotti G., Danese, L. 2008, ApJ, 689, L101
 Fontana, A. et al. 2009, A&A, 501, 15
 Hyde J.B., Bernardi M. 2009, MNRAS, 394, 1978
 Hopkins P.F., Bundy K., Murray N., Quataert E., Lauer T.R., Ma C.-P. 2009, MNRAS, 398, 898
 Khochfar S. & Silk J. 2006, MNRAS, 370, 902
 Kriek, M. et al. 2006, ApJ, L71
 Laureijs R. et al. 2011, Euclid Definition Study Report (arXiv:1110.3193)
 Lotz J. M., Jonsson P., Cox T. J., Croton D., Primack J. R., Somerville R. S., Stewart K., 2011, ApJ, in press (arXiv:1108.2508)
 Mancini, C.; Daddi, E.; Renzini, A. et al. 2010, MNRAS, 401, 933
 Maraston C. 2005, MNRAS, 362, 799
 Moresco M. et al. 2010, A&A, 524, 67
 Naab T., Johansson P.H., Ostriker J.P. 2009, ApJ, 699, L178
 Newman A.B., Ellis R.S.; Bundy K., Treu T. 2011, ApJ, in press (arXiv:1110.1637)
 Nipoti C., Londrillo P., Ciotti L., 2003, MNRAS, 342, 501
 Nipoti C., Treu T., Bolton A. S., 2009a, ApJ, 703, 1531
 Nipoti C., Treu T., Auger M.W., Bolton A.S. 2009b, ApJ, 706, L86
 Nipoti C., Treu T., Leauthaud A., Bundy K., Newman A. B., Auger M. W., 2012, MNRAS in press (arXiv:1202.0971)
 Onodera M. et al. 2010, ApJ, 715, L60
 Oser L., Naab T., Ostriker J.P., Johansson P.H. 2011, ApJ, in press (arXiv:1106.5490)
 Papovich C. et al. 2011, ApJ, in press (arXiv:1110.3794)
 Pforr J., Maraston C., Tonini C. 2012, MNRAS, submitted
 Pozzetti, L. et al. 2010, A&A, 523, 13
 Ragone-Figueroa C., Granato G. L., 2011, MNRAS, 414, 3690
 Renzini A., 2006, ARA&A, 44, 141
 Rettura A. et al. 2010, ApJ, 709, 512
 Scarlata C. et al. 2007, ApJS, 172, 406
 Saglia R.P. et al. 2010, A&A, 524, 6
 Saracco P., Longhetti, M., Andreon, S. 2009, MNRAS, 392, 718
 Shen S. et al. 2003, MNRAS, 343, 978
 Shih H.-Y., Stockton A. 2011, ApJ, 733, 45
 Springel V., et al., 2005, Nature, 435, 629
 Strazzullo V. et al. 2010, A&A, 524, 17
 Taylor E.N., Franx M., Glazebrook K., Brinchmann J., van der Wel A., van Dokkum P.G. 2010, ApJ, 720, 723
 Trujillo I. et al. 2006, MNRAS, 373, L36 2006, MNRAS, 373, L36
 Valentinuzzi T. et al. 2010, ApJ, 721, L19
 van de Sande J. et al. 2011, ApJ, 736, L9
 van der Wel A. et al. 2008, ApJ, 688, 48
 van der Wel A. et al. 2011, ApJ, 730, 38
 van Dokkum P.G. et al. 2008, ApJ, 677, L5
 van Dokkum P.G., Kriek M., Franx, M. 2009, Nature, 460, 717
 van Dokkum P.G., Brammer G. 2010, ApJ, 718, L73
 Williams R.J., Quadri R.F., Franx M., van Dokkum P., Toft S., Kriek M., Labbe I. 2010, 713, 738